Supplemental Material For:

Identification of MltG as a potential terminase for peptidoglycan polymerization in bacteria

Rachel Yunck[1], Hongbaek Cho[1], and Thomas G. Bernhardt[1*]

[1]Department of Microbiology and Immunobiology
Harvard Medical School
Boston, MA 02115

*To whom correspondence should be addressed.
Thomas G. Bernhardt, Ph.D.
Harvard Medical School
Department of Microbiology and Immunobiology
Boston, Massachusetts 02115
e-mail: thomas_bernhardt@hms.harvard.edu

SUPPLEMENTAL FIGURE LEGENDS

Figure S1. MltG generates muropeptides with non-reducing termini. Extracted-ion chromatogram for 922.38 *m/z* (see **Figure 5A**) and Total-ion chromatograms (TIC) resulting from the digestion of purified, unlabeled PG with MltG. **(B)** and **(C)** chromatograms compare the total products observed with and without sodium borohydride reduction, which reduces the MurNAc sugar in a GlcNAc-MurNAc disaccharide to muramitol. If there is a free reducing end, there will be a 2 Da difference after reduction and a slight shift in retention time. If there is no reducing end, the products will not shift in mass and there will be no observed shift in retention time. **(A)** Products corresponding to 922.389 m/z align with the primary peaks in the TIC **(B**). These peaks do not shift in mass or retention time with reduction indicating that the three primary products generated by MltG have non-reducing termini, a property consistent with muropeptides that lack a free N-acetylmuramic acid and are capped by 1,6-anhydro-*N*-acetylmuramic acid. As shown in the inset in **(A)**, two possible products could result in the same *m/z* ratio of 922.38 with *z*=2, *one* oligomeric and one cross-linked. However, the cross-linked product has a reducing end (indicated by the *), whereas the oligomeric product with the anhydro cap does not. Therefore, only the oligomeric product would resist reduction as observed with the larger products generated by MltG. A similar pattern and conclusion has been observed for the products released by MltE, a previously characterized endo-acting lytic transglycosylase (Lee *et al.*, 2013).

Figure S2. Conservation profiles of MltG and other LTs. A. Graph showing the number of genomes in which each LT family is found out of the total 150 used in the diversity set. **B.** Graph showing the percentage of gram-negative vs gram-positive organisms in the dataset

containing each LT family. **D.** Table outlining the primary Pfams found in each family of LTs. These Pfams were used to identify potential members of each LT family analyzed in **Figure 6.**

Figure S3. Total ion chromatogram resulting from the mutanolysin digestion of unlabeled, purified PG isolated from WT (TB28) or Δ*mltG* (RY36). The inset shows a zoomed-in view of the region with the peak corresponding to GM-pentapeptide. The peak labels correspond with the peaks identified and quantified in **Table S1.**

Figure S3. Overlaid chromatograms showing the peaks associated with peptide-free glycan strands released from AmiD-treated sacculi isolated from WT (TB28, black) and Δ*mltG* (RY36, red). The resulting peptide-free glycan strands were then separated according to length using a previously described HPLC protocol (Harz *et al.*, 1990). Peaks increase in length with increasing elution times. However, here, the precise number of disaccharides per peak was not determined as the HPLC conditions were incompatible with mass spectrometry. The integrated area under the peaks numbered 1-26 correspond with the graph shown **Figure 8C.**

Figure S5. Putative LysM domain in MltG (A) The Phyre2 server (Kelley *et al.*, 2015) predicted the presence of a LysM-like domain near the N-terminus of MltG, in a region that was not structurally characterized in *E. coli* MltG. However, the structure of the LysM-like region of MltG in *Listeria monocytogenes* has been solved (PDB: 4iiw). Shown is the Phyre2 alignment of the canonical LysM domain from MltD with the predicted secondary structure and amino acid sequence of $MltG^{E.\ coli}$ and the known secondary structure and sequence of $MltG^{Listeria}$. The degree of conservation of each residue in this region of MltG is shown as a

color coded box underneath each residue, determined using the Consurf server (Ashkenazy *et al.*, 2010). An asterisk (*) marks the putative ligand binding domain important for PG binding (Bateman and Bycroft, 2000). The color legend for conservation is shown in **(C). (B)** Cartoons of the crystal structures of the LysM domain from MltD (PDB:1E0G) and the predicted LysM-like domain of MltG from *L. monocytogenes* (PDB: 4iiw). **(C)** Shown is a space-filling model of the MltG structure from *L. monocytogenes* (PDB 4iiw) colored to indicate amino acid conservation using ConSurf (Ashkenazy *et al.*, 2010). Note the high conservation of residues in the cleft-forming region that aligns with the known catalytic region of MltG from *E. coli* as well as the high degree of conservation near the N-terminus in a cleft coinciding with the putative LysM-like domain. This LysM-like domain resides close to the predicted transmembrane region of MltG.

Table S1. Muropeptide analysis. Table listing the major muropeptide species identified by LCMS following mutanolysin digest of WT (TB28) or *ΔmltG* (RY36) sacculi. Peak numbers correspond to the labeled peaks shown in **Figure S3.** GM^R indicates a GlcNAc-MurNAc disaccharide with the MurNAc sugar reduced to muramitol for the LCMS analysis. Peptide length is given following the dash (-) and crosslinks are indicated with a slash (/). Peaks marked with a (*) could correspond with either the shown species (A / B) or the reciprocal dimer (B / A). The percent of total of muropeptides was calculated from the extracted ion counts for each muropeptide species after normalization for total muropeptide levels in each sample. Percent change was calculated by the following formula: [% Area (*ΔmltG*) - % Area (WT)] / % Area (WT) * 100. All values were determined through analysis of three biological replicates from sacculi isolated from cultures grown from independent colonies. Other minor

muropeptides species not shown in the table were also identified and included in the summary calculations shown in **Figure 8** and **Table S2.**

Table S2. Table summarizing the major categories of muropeptides, organized by (**A)** glycan composition and cross-linkage and (**B)** stem peptide composition and cross-linkage. Values represent percentage of total muropeptides calculated from the LCMS muropeptide analysis described in **Figure 8** and **Table S1 / Figure S4**.

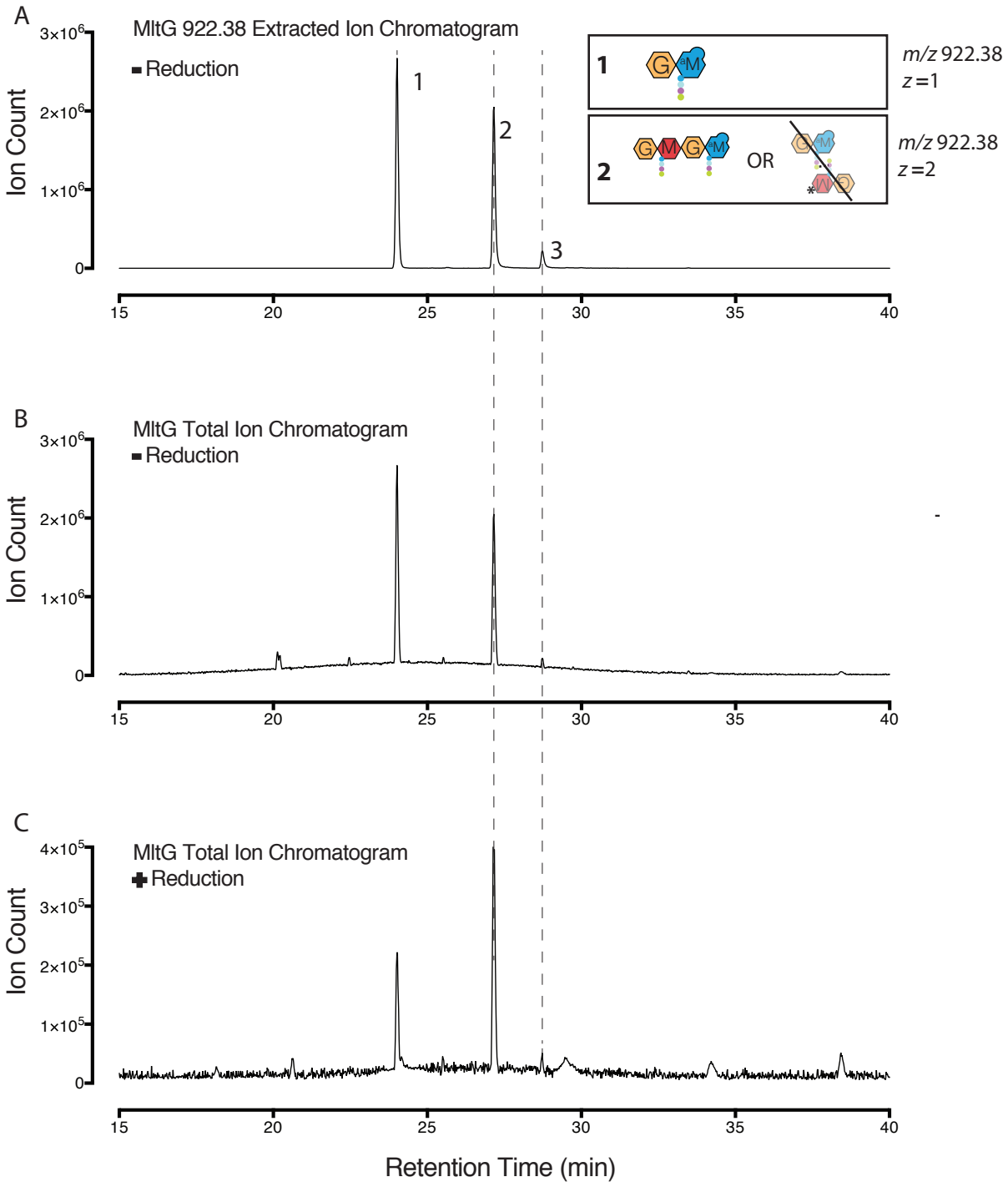
A
MltG 922.38 Extracted Ion Chromatogram
Reduction
Ion Count
3×10^6
2×10^6
1×10^6
0
1
2
3
m/z 922.38
z =1
m/z 922.38
z =2
OR
15
20
25
30
35
40
B
MltG Total Ion Chromatogram
Reduction
C
MltG Total Ion Chromatogram
Reduction
4×10^5
3×10^5
2×10^5
1×10^5
Retention Time (min)

Figure S1

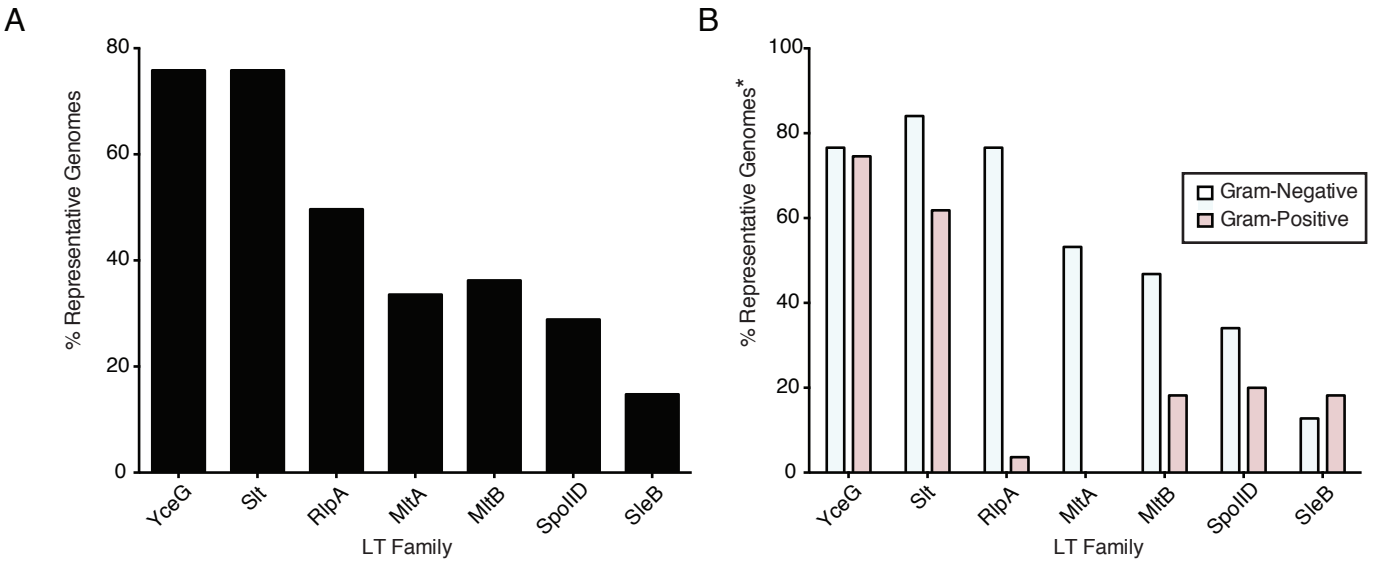

LT Family	Pfam Identifier	Pfam Name
Slt	PF01464	Transglycosylase SLT domain
MltG	PF02618	YceG-Like domain
MltA	PF03562 (w/ PF06725)	MltA specific insert domain
MltB	PF13406	SLT_2: Transglycosylase SLT domain
RlpA	PF03330	DPBB_1: Rare lipoprotein A (RlpA)-like double-psi beta-barrel
SleB	PF07486	Hydrolase_2: Cell Wall Hydrolase
SpoIID	PF08486	SpoIID: Stage II sporulation protein

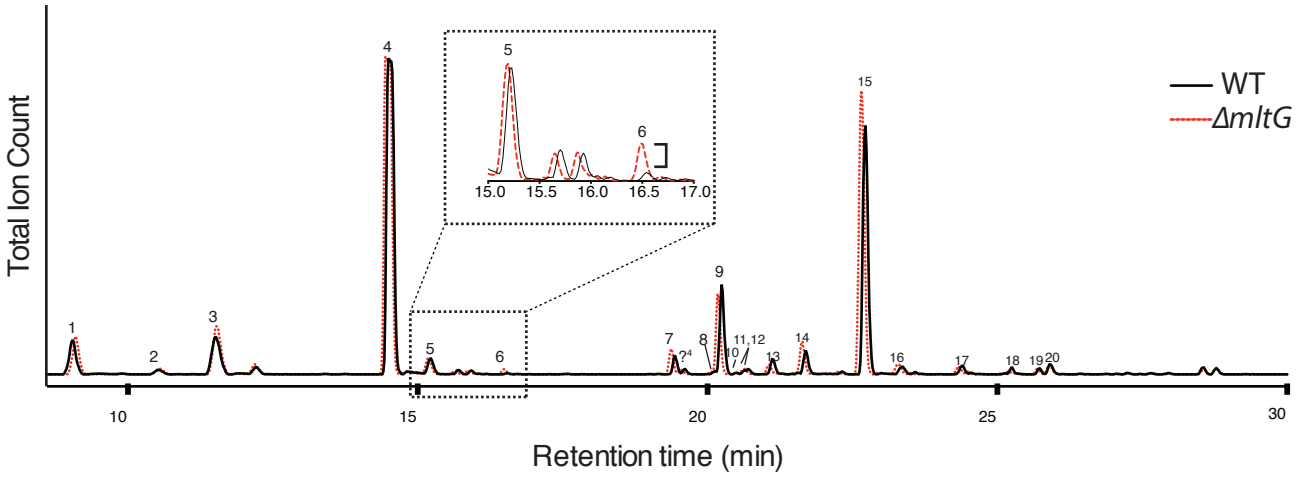
Total Ion Count
Retention time (min)
WT
ΔmltG
1
2
3
4
5
6
7
8
9
10
11,12
13
14
15
16
17
18
19
20
10
15
20
25
30
15.0
15.5
16.0
16.5
17.0

Figure S3

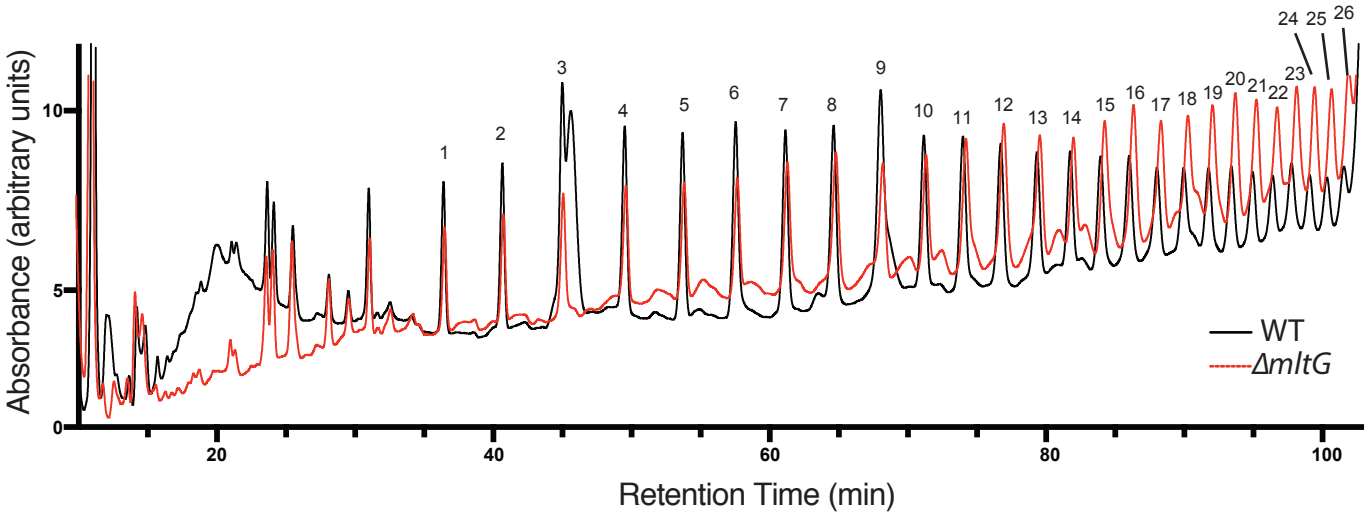
Absorbance (arbitrary units)
0
5
10
20
40
60
80
100
Retention Time (min)
1
2
3
4
5
6
7
8
9
10
11
12
13
14
15
16
17
18
19
20
21
22
23
24
25
26
WT
ΔmltG

Figure S4

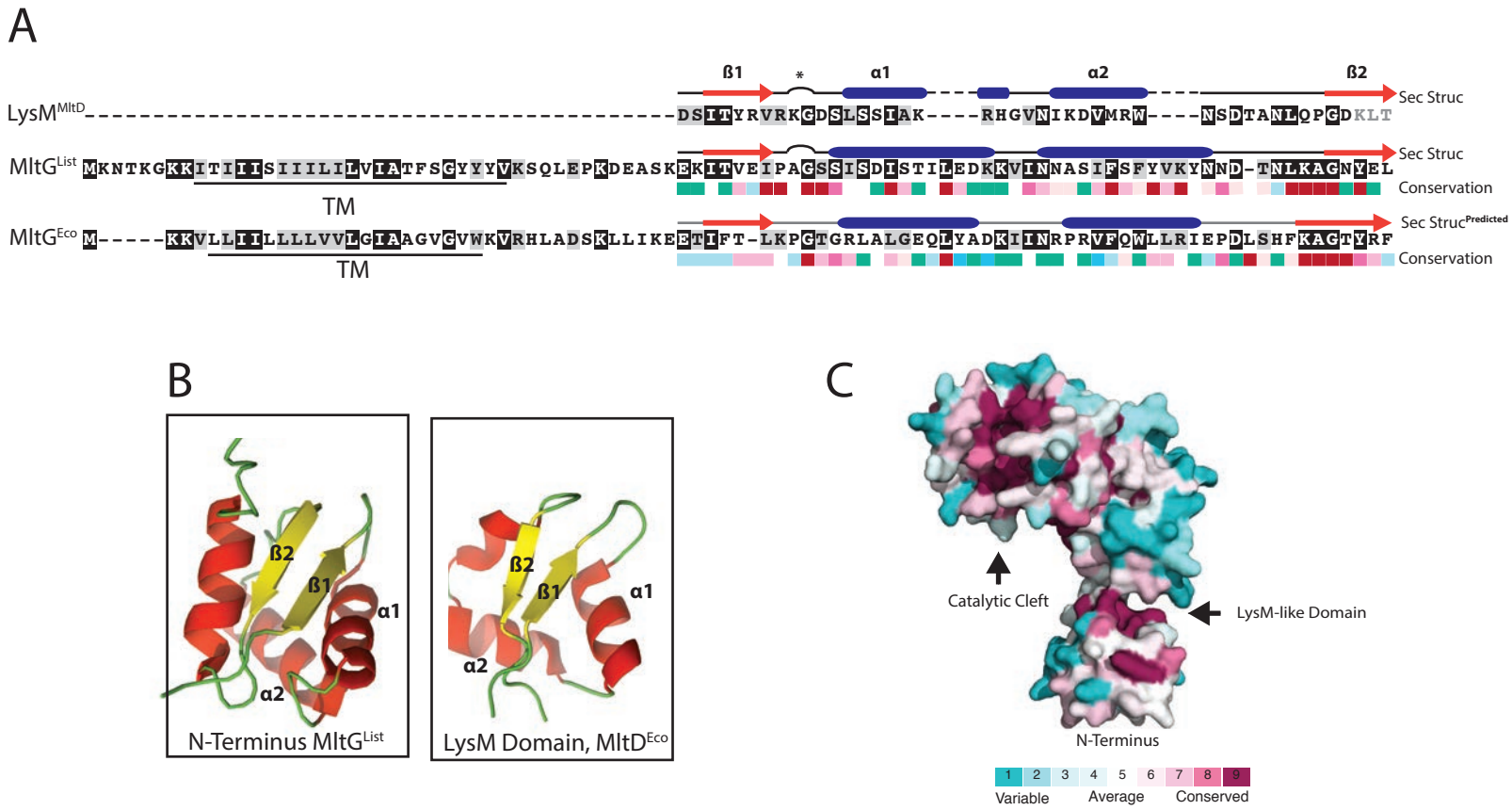
A
ß1
*
α1
α2
ß2
LysM^MltD
Sec Struc
MltG^List
TM
Conservation
MltG^Eco
Sec Struc^Predicted
B
ß2
ß1
α1
α2
N-Terminus MltG^List
LysM Domain, MltD^Eco
C
Catalytic Cleft
LysM-like Domain
N-Terminus
1 2 3 4 5 6 7 8 9
Variable
Average
Conserved

Figure S5

Table 1. Muropeptide analysis.

Peak	Identity	RT (min)	Exact Mass	Observed m/z [M+H$^+$]	Theoretical m/z [M+H$^+$]	z	WT % Total Peak Area ± SD	Δ*mltG* % Total Peak Area ± SD	% Δ	P Value
1	GM ^{R}-Tri	9.1	870.37	871.37	871.37	+1	7.54 ± 0.19	7.00 ± 0.32	-7.16	
2	GM ^{R}-Tri-Gly(4)	10.6	927.39	928.40	928.4 464.70	+1 +2	1.76 ± 0.11	1.92% ± 0.08	9.09	
3	GM ^{R}-Tri-Lys(4)-Arg(5)	11.6	1154.57	578.29	578.29	+2	11.12 ± 0.71	10.63 ± 0.51	-4.38	
4	GM ^{R}-Tetra	14.5	941.41	942.41 471.71	942.41 471.71	+1 +2	38.19 ± 0.92	39.46 ± 0.48	3.32	
5	GM ^{R}-Di	15.2	698.29	699.29	699.29	+1	1.73 ± 0.12	1.52 ± 0.06	-12.33	
6	GM ^{R}-Penta	16.6	1012.44	1013.45 507.23	1013.45 507.23	+1 +2	0.09 ± 0.01	0.32 ± 0.05	251.9	p<0.01
7	GM ^{R}-Tri/ GM ^{R}-Tri-Lys(4)-Arg(5), $^{3-3}$	19.4	2006.93	669.98	669.98	+3	0.83 ± 0.06	0.98 ± 0.06	15.3	
8	GM ^{R}-Tri / GM ^{R}-Tri $^{R, 3-3}$	20.1	1722.73	862.37	862.37	+2	0.41 ± 0.02	0.38 ± 0.03	-7.9	
9*	GM ^{R}-Tetra / GM ^{R}-Tri-Lys(4)-Arg(5) $^{4-3}$	20.2	2077.96	694.00	693.66	+3	4.80 ± 0.18	4.13 ± 0.21	-13.96	
10	GAnhM-Tri-Lys-Arg	20.5	1134.54	568.28	568.28	+2	0.16 ± 0.00	0.15 ± 0.01	-6.7	
11	GAnhM-Tri	20.6	850.34	851.35	851.35	+1	0.36 ± 0.01	0.26 ± 0.02	-27.1	p<0.01
12*	GM ^{R}-Tetra / GM ^{R}-Tri-Gly(4) $^{4-3}$	20.7	1850.79	926.4	926.4	+2	0.69 ± 0.03	0.65 ± 0.03	-4.8	
13*	GM ^{R}-Tri / GM ^{R}-Tetra $^{3-3}$	21.1	1793.77	897.89	897.89	+2	1.92 ± 0.05	1.23 ± 0.08	-36.11	p<0.01
14*	GM ^{R}-Tetra / GM ^{R}-Tri $^{4-3}$	21.7	1793.77	897.89	897.89	+2	3.08 ± 0.14	3.80 ± 0.17	23.73	
15	GM ^{R}-Tetra / GM ^{R}-Tetra $^{4-3}$	22.7	1844.78	933.41	933.41	+2	18.25 ± 0.60	19.33 ± 0.35	5.9	
16a	GM ^{R}-Tetra / Penta	23.3	1455.65	729.32	729.32	+2	0.61 ± 0.02	0.74 ± 0.01	19.57	p<0.01
16b	GM ^{R}-Tetra / GM ^{R}-Penta $^{4-3}$	23.4	1935.84	968.93 646.29	968.42 646.29	+2 +3	0.12 ± 0.00	0.16 ± 0.01	36.11	
17	GAnhM-Tetra	24.4	921.38	922.39 461.70	922.39 461.70	+1 +2	0.82 ± 0.03	0.72 ± 0.05	-12.25	

Table S2 Summary of the muropeptide composition of WT and Δ*mltG* sacculi

A

	WT	Δ*mltG*	% Δ
Un-crosslinked	**60.01%**	**60.05%**	**0.07%**
GM	58.68%	58.93%	0.43%
GAnhM	1.33%	1.12%	-15.79%
Dimers	**31.95%**	**32.17%**	**0.69%**
GM/GM	30.02%	30.75%	2.43%
GM/GAnhM	1.93%	1.42%	-26.42%
Trimers	**1.47%**	**1.23%**	**-16.33%**
GM/GM/GM	1.26%	1.12%	-11.11%
GAnhM/GM/GM	0.21%	0.12%	-42.86%
All GM	**91.07%**	**91.59%**	**0.57%**
All GAnhM	**2.37%**	**1.87%**	**-21.10%**

B

	WT	Δ*mltG*	% Δ
Tri	**11.26%**	**10.67%**	**-5.24%**
Monomer	7.90%	7.30%	-7.59%
Dimer	3.30%	3.40%	3.03%
Trimer	0.03%	0.04%	33.33%
Tri-Lys-Arg	**23.49%**	**21.60%**	**-8.05%**
Monomer	11.28%	10.78%	-4.43%
Dimer	12.12%	10.76%	-11.22%
Trimer	0.10%	0.06%	-37.76%
Tetra	**65.37%**	**66.06%**	**1.06%**
Monomer	39.01%	39.46%	1.16%
Dimers	25.02%	25.47%	1.77%
Trimers	1.34%	1.13%	-15.38%
Penta	**0.46%**	**0.77%**	**67.39%**
Monomer	0.09%	0.32%	255.56%
Dimers	0.37%	0.45%	21.62%

Table S3. Strains used in this study

Strain	Genotype[a]	Source/Reference[b]
BTH101	*cya-99 araD139 galE15 galK16 rpsL1 (*Str^R*), hsdR2, mcrA1, mcrB1, relA1*	Euromedex
BW25113	*Δ(araD-araB)567 ΔlacZ4787(::rrnB-3) rph-1 Δ(rhaD-rhaB)568 hsdR514*	(Baba *et al.*, 2006)
DH5α	*F– hsdR17 deoR recA1 endA1 phoA supE44 thi-1 gyrA96 relA1 Δ(lacZYA-argF)U169 φ80dlacZΔM15*	Gibco BRL
JW1083	BW25113 Δ*yceG761*::Kan^R	(Baba *et al.*, 2006)
MG1655	*rph-1 ilvG rfb-50*	(Guyer *et al.*, 1981)
Rosetta2(λDE3)	F$^-$ *ompT hsdS*$_B$(r$_B^-$ m$_B^-$) *gal dcm* (DE3) pRARE2 (Cm^R)	Novagen
HC419	TB28 Δ*lysA763*::*frt* Δ*ampD728*::*frt* Δ*slt*::Kan^R	(Cho *et al.*, 2014)
NP140	TB28 Δlpp	TU163/pCP20
RY8	TB28 Δ*mltG*::Kan^R	P1(JW1083)xTB28
RY34	TB10 Δ*mltG*::Cm^R	λRed
RY35	TB28 Δ*mltG*::Cm^R	P1(RY34) x TB28
RY36	TB28 Δ*mltG*::*frt*	RY35/pCP20
RY43	TB28 Δ*lysA763*::*frt* Δ*ampD728*::*frt* Δ*mltG::*Cm^R	P1(RY34) x TU278
RY44	TB28 Δ*lysA763*::*frt* Δ*ampD728*::*frt* Δ*slt*:: Kan^R *ΔmltG::*Cm^R	P1(JW1083) x TB28
TB10	*rph-1 ilvG rfb-50* λΔ*cro-bio nad*::Tn10	(Johnson *et al.*, 2004)
TB28	MG1655 Δ*lacIZYA*::*frt*	(Bernhardt and de Boer, 2004)
TU122	TB28 Δ*ponB(mrcB)*::*frt*	(Paradis-Bleau *et al.*, 2010)
TU163	TB28 Δ*lpp*::Kan^R	{Uehara:2010cp}
TU278	TB28 Δ*lysA763*::*frt* Δ*ampD728*::*frt*	(Cho *et al.*, 2014)

[a] The Kan^R and Cm^R cassettes are flanked by *frt* sites for removal by FLP recombinase. An *frt* scar remains following removal of the cassette using FLP expressed from pCP20.

[b] Strain constructions by P1 transduction are described using the shorthand: P1(donor) x recipient. Transductants were selected on LB Kan or Cam plates where appropriate. Strains resulting from the removal of frt-flanked antibiotic resistance gene using pCP20 are indicated as: Parental strain/pCP20. λRed indicates strains were constructed by recombineering (see Experimental Procedures for details).

Table S4. Plasmids used in this study.

Plasmid	Genotype[a]	Origin	Source/Reference
pCM6	*cat* P_{ara}::*empty*	p15A	This study
pCP20	*bla cat c*I875 *repA*(Ts) P_R::*flp*	pSC101	(Datsenko and Wanner, 2000)
pDY1	*cat lacI*^{q} P_{lac}::*ponB lacZ*	mini-F	This study
pInt-ts	*bla c*I875 *repA*(Ts) P_R::*int*$^{\lambda}$	pSC101	(Haldimann and Wanner, 2001)
pMM47	*att*HK022 *bla lacI*^{q} P_{lac}::^{ss}*pal-mcherry*	R6K	(Paradis-Bleau *et al.*, 2010)
pNP8	*att*HK022 *bla lacI*^{q} P_{lac}::*mltG*	R6K	This study
pNP9	*att*HK022 *bla lacI*^{q} P_{lac}::*mltG-mcherry*	R6K	This study
pRY30	*cat* P_{ara}:: MG1655 loci (1153098-1154818)	p15A	Screen Isolate genomic coordinates of insert are indicated
pRY42	*cat lacI*^{q} P_{lac}::*mltG*	pBR/colE1	This study
pRY47	*cat lacI*^{q} P_{lac}::*empty*	pBR/colE1	(Cho *et al.*, 2014)
pRY53	*cat* P_{ara}::*mltG*	p15A	This study
pRY54	*bla lacI*^{q} P_{T7}::*h-sumo-s-mltG*	pBR/colE1	This study
pRY62	*bla lacI*^{q} P_{T7}::*h-sumo-s-mltG(E218Q)*	pBR/colE1	This study
pRY66	*cat lacI*^{q} P_{lac}::*mltG (S138C)*	pBR/colE1	This study
pRY68	*cat lacI*^{q} P_{lac}::*mltG (A19C)*	pBR/colE1	This study
pRY70	*cat lacI*^{q} P_{lac}::*mltG (K3C)*	pBR/colE1	This study
pRY77	*att*HK022 *bla lacI*^{q} P_{lac}::^{ss}*pal*(D^{+2} E^{+3})*-mcherry*	R6K	This study
pRY78	*bla lacI*^{q} P_{lac}::*T18-mltG*	pBR/colE1	This study
pRY79	*aph* P_{lac}::*T25-mltG*	p15A	This study
pRY86	*bla lacI*^{q} P_{lac}::*T18-ponA*	pBR/colE1	This study
pRY87	*aph* P_{lac}::*T25-ponA*	p15A	This study
pRY88	*bla lacI*^{q} P_{lac}::*T18-ponB*	pBR/colE1	This study

Plasmid	Genotype[a]	Origin	Source/Reference
pRY89	*aph* P_{lac}::*T25-ponB*	p15A	This study
pTB102	*cat c*I875 *repA*(Ts) P_R::int^{HK022}	pSC101	(Bernhardt and de Boer, 2005)
pTB145	*bla lacI*^{q} P_{T7}::*h-ulp1(403-621)*	pBR/colE1	(Bendezú and de Boer, 2008)
pTB146	*bla lacI*^{q} P_{T7}::h-sumo	pBR/colE1	(Bendezú and de Boer, 2008)
pTU136	*att*HK022 *bla lacI*^{q} P_{lac}::^{ss}*dsbA-mCherry*	R6K	(Uehara *et al.*, 2009)
pUT18-zip	*bla lacI*^{q} P_{lac}::*T18-zip*	p15A	Euromedex
pKT25-zip	*aph* P_{lac}::*T25-zip*	pBR/colE1	Euromedex

[a] A 6xHis tag for purification is indicated by the letter *h*. ^{ss}*dsbA* corresponds to the first 24 codons of *dsbA* encoding its export signal. P_{lac}, P_{T7}, P_R, and P_{ara} indicate the lactose, phage T7, λR and arabinose promoters, respectively. Numbers in parenthesis indicate the codons included in the relevant clones.

Plasmid Construction

pCM6

The plasmid pCM6 [*cat* P_{ara}::*empty*] was constructed as follows. The pBAD33 vector (Guzman *et al.*, 1995) was modified by Quick-Change site-directed mutagenesis to remove the BamHI site located in the arabinose promoter region using the primers 5'-ATCCATAAGATTAGCGAATCCTACCTGACGC-3' and 5'-GCGTCAGGTAGGATTCGCTAATCTTATGGAT-3' according to standard procedures.

pDY1

The plasmid pDY1 [*bla lacI*^{q} P_{lac}::*ponB lacZ*] was constructed as follows. The primers 5'-GTCA***GAATTC***GGGCTTTTGCGCCTGAATATTG-3' and 5'-GTCA***CTCGAG***ATGGGATGTTA TTTTACCGGATGGC-3' were used to amplify *ponB* from pTU110 (Paradis-Bleau *et al.*, 2010). The resulting PCR product was purified, digested with EcoRI and XhoI, and ligated into pRC7 (de Boer *et al.*, 1989) digested with EcoRI and SalI.

pNP8

The plasmid pNP8 [*att*HK022 *bla lacI*^{q} P_{lac}::*mltG*] was constructed as follows. The primers 5'-GTAC***AAGCTT***TTACTGCGCATTTTTTTCCTTAAGCACTTTC-3' and 5'-GTAC***TCTAGA***TTTA AGGAGGTGATATACATATGAAAAAAGTGTTATTGATAATCTTG TTATTGCTGGTG-3' were used to amplify *mltG* from E. coli MG1655 genomic DNA. The resulting PCR product was purified, digested with XbaI and HindIII, and ligated into similarly digested pTB225 (Uehara *et al.*, 2009).

pNP9

The plasmid pNP9 [*att*HK022 *bla lacI*^{q} P_{lac}::*mltG-mcherry*] was constructed as follows. The primers 5'-GTAC***TCTAGA***TTTAAGGAGGTGATATACATATGAAAAAAGTGTTATTGATAATCTTG TTATTGCTGGTG-3' and 5'-CTTCTGA***CTCGAG***CTGCGCATTTTTTTCCTTAAGCACTT

TCAG-3' were used to amplify *mltG* from E. coli MG1655 genomic DNA. The resulting PCR product was purified, digested with XbaI and XhoI, and ligated into similarly digested pNP3 (Peters *et al.*, 2011).

pRY42

The plasmid pRY42 [*cat lacI*^{q} P_{lac}::*mltG*] was constructed as follows. The *mltG* containing XbaI/HindIII fragment of pNP8 [*att*HK022 *bla lacI*^{q} P_{lac}::*mltG*] was used to replace the corresponding fragment of pTU272 [*cat lacI*^{q} P_{lac}::*slmA*].

pRY52

The plasmid pRY52 [*cat* P_{ara}::*mltG(E218Q)*] was constructed as follows. The internal primers 5'-TGGCATCAATTATCGAAAAACAAACCGCCGTTGCCAGTGAACGC-3' , 5'-GCGTTCACTGGCAACGGCGGTTTGTTTTTCGATAATTGATGCCA-3'
and the external primers 5'-GTAC***TCTAGA***TTTAAGGAGGTGATATACATATGAAAAAAGTGTTA TTGATAATCTTGTTATTGCTGGTG-3', 5'-GTAC***AAGCTT***TTACTGCGCATTTTTTTC CTTAAGCACTTTC-3' were used in overlap extension PCR to amplify *mltG* from genomic DNA and to perform site directed mutagenesis to create the E218Q mutation in the *mltG* gene. The resulting PCR product was purified, digested with XbaI and HindIII, and ligated into similarly digested pTB285 (Uehara *et al.*, 2010).

pRY53

The plasmid pRY53 [*cat* P_{ara}::*mltG*] was constructed as follows. The *mltG* containing XbaI/HindIII fragment of pNP8 [*att*HK022 *bla lacI*^{q} P_{lac}::*mltG*] was used to replace the corresponding fragment of pCM6.

pRY54

The plasmid pRY54 [*bla lacI*^{q} P_{T7}::*h-sumo-s-mltG*] was constructed as follows. The primers 5'-GTCA***GGATCC***CGCCATCTTGCCGACAGCAAATTGC-3' and 5'-GTAC***AAGCTT***TTACTGC GCATTTTTTTCCTTAAGCACTTTC-3' were used to amplify *mltG* from pNP8. The resulting PCR product was purified, digested with HindIII and BamHI-HF, and ligated into similarly digested pTD68 (Morlot *et al.*, 2010).

pRY62

The plasmid pRY62 [*bla lacI*^{q} P_{T7}::*h-sumo-s-mltG(E218Q)*] was constructed as follows. The primers 5'-GTCA***GGATCC***CGCCATCTTGCCGACAGCAAATTGC-3' and 5'-GTAC***AAGCTT***TTACTGCGCATTTTTTTCCTTAAGCACTTTC-3' were used to amplify *mltG (E218Q)*$^{27\text{-}340}$ from pRY52. The resulting PCR product was purified, digested with HindIII/BamHI-HF, and ligated into pTD68 (Morlot *et al.*, 2010).

pRY66

The plasmid pRY66 [*cat lacI*^{q} P_{lac}::*mltG (S138C)*] was constructed as follows. The internal primers 5'-CGTATATCAAGCATACGCTGTGCGATGATAAGTACGCCACC-3', 5'-GGTGGCGTACTTATCATCGCACAGCGTATGCTTGATATACG-3' and external primers 5'-GTAC***TCTAGA***TTTAAGGAGGTGATATACATATGAAAAAAGTGTTATTGATAATCTTGTTATTGCTGGTG-3', 5'-GTAC***AAGCTT***TTACTGCGCATTTTTTTCCTTAAGCACTTTC-3' were used in overlap extension PCR to amplify *mltG* from genomic DNA and to perform site directed mutagenesis to create the S138C mutation in the *mltG* gene. The resulting PCR product was purified, digested with XbaI and HindIII, and ligated into similarly digested pTU272 [*cat lacI*^{q} P_{lac}::*slmA*].

pRY68

The plasmid pRY68 [*cat lacI*^{q} P_{lac}::*mltG (A19C)*] was constructed as follows. The internal primers 5'-TGGTGGTACTGGGTATCGCCTGTGGTGTGGGCGTCTGGAAGG-3', 5'-CCTTCCAGACGCCCACACCACAGGCGATACCCAGTACCACCA-3' and the external primers 5'-GTAC***TCTAGA***TTTAAGGAGGTGATATACATATGAAAAAAGTGTTATTGATAATCTTGTTAT TGCTGGTG-3', 5'-GTAC***AAGCTT***TTACTGCGCATTTTTTTCCTTAAGCACTTTC-3' were used in overlap extension PCR to amplify *mltG* from genomic DNA and to perform site directed mutagenesis to create the A19C mutation in the *mltG* gene. The resulting PCR product was purified, digested with XbaI and HindIII, and ligated into similarly digested pTU272 [*cat lacI*^{q} P_{lac}::*slmA*].

pRY70

The plasmid pRY70 [*cat lacI*^{q} P_{lac}::*mltG (K3C)*] was constructed as follows. The internal primers 5'-GAGGTGATATACATATGAAATGCGTGTTATTGATAATCTTGTT-3', 5'-AACAAGATTATCAATA ACACGCATTTCATATGTATATCACCTC-3' and the external primers 5'-GTAC***TCTAGA***TTTAAG GAGGTGATATACATATGAAAAAAGTGTTATTGATAATCTTGTTATTGCTGGTG-3', 5'-GTAC ***AAGCTT***TTACTGCGCATTTTTTTCCTTAAGCACTTTC-3' were used in overlap extension PCR to amplify *mltG* from genomic DNA and to perform site directed mutagenesis to create the K3C mutation in the *mltG* gene. The resulting PCR product was purified, digested with XbaI and HindIII, and ligated into similarly digested pTU272 [*cat lacI*^{q} P_{lac}::*slmA*].

pRY77

The plasmid pRY77 [*att*HK022 *bla lacI*^{q} P_{lac}::^{ss}*pal(D*$^{+2}$ *E*$^{+3}$*)-mcherry*] was constructed as follows. The gene fragment encoding ^{ss}*pal(D*$^{+2}$ *E*$^{+3}$*)* GTAC***TCTAGA***AATAATTTTGTTTAACTTTAAGAAG GAGATATACATATGCAACTGAACAAAGTGCTGAAAGGGCTGATGATTGCTCTGCCTGTTATGGCAAT TGCGGCATGTGATGAGAACAAGAACGCC***CTCGAG***GTAC was synthesized as a gBlock by

Integrated DNA Technologies (IDT). This gBlock was digested with XbaI and XhoI, and ligated into similarly digested pMM46 (Paradis-Bleau *et al.*, 2010).

pRY78

The plasmid pRY78 [*bla lacI*^{q} P$_{lac}$::*T18-mltG*] was constructed as follows. The primers 5'-GTAC***GGATCC***AAAAAAGTGTTATTGATAATCTTGTTATTG-3' and 5'- GTCA***CTCGAG***TTACTG CGCATTTTTTTCCTTAAGC-3' were used to amplify *mltG* from pRY42. The resulting PCR product was purified, digested with BamHI-HF / XhoI, and ligated into similarly digested pTU234 [*bla lacI*^{q} P$_{lac}$::*T18-amiA*].

pRY79

The plasmid pRY79 [*aph* P$_{lac}$::*T25-mltG*] was constructed as follows. The primers 5'-GTAC***GGATCC***AAAAAAGTGTTATTGATAATCTTGTTATTG-3' and 5'- GTCA***CTCGAG***TTACTG CGCATTTTTTTCCTTAAGC-3' were used to amplify *mltG* from pRY42. The resulting PCR product was purified, digested with BamHI-HF / XhoI, and ligated into similarly digested pTU235 [*aph* P$_{lac}$::*T25-amiA*].

pRY86

The plasmid pRY86 [*bla lacI*^{q} P$_{lac}$::*T18-ponA*] was constructed in several steps as follows. The primers 5'-AGGTCGACTCTAGAA***GGATCC***AAGTTCGTAAAGTATTTTTTGATC-3' and 5'-GAGCTCAAGCTTATTACTCAGAACAATTCCTGTGC-3' were used to amplify *ponA* from E. coli MG1655 genomic DNA. Using isothermal assembly, the resulting PCR fragment was incorporated into the corresponding fragment of BamHI-HF/XhoI digested pRY78.

pRY87

The plasmid pRY87 [*aph* P_{lac}::*T25-ponA*] was constructed as follows. First, the primers 5'-AGGTCGACTCTAGAA***GGATCC***AAGTTCGTAAAGTATTTTTTGATC-3', 5'-GGAACAATTCCTG TGCCTCGCCATTATC-3' were used to amplify *ponA* from E. coli MG1655 genomic DNA. In a second PCR reaction, the primers 5'-AGGTCGACTCTAGAA***GGATCC***AAGTTCGTAAAGTATTT TTTGATC-3' and 5'-***TCGAG***GAACAATTCCTGTGCCTCGCCATTATC-3' were used to amplify *ponA* with a 3' XhoI restriction site. *ponA* contains an internal XhoI restriction site, so instead of digesting with XhoI, the two PCR products were mixed and annealed to create an overhang similar to that obtained with XhoI digestion (C/***TCGAG***). The resulting product was purified, digested with BamHI-HF, and ligated into BamHI-HF/XhoI digested pRY79.

pRY88

The plasmid pRY88 [*bla lacI*^{q} P_{lac}::*T18-ponB*] was constructed as follows. The primers 5'-GGGTCGACTCTAGAA***GGATCC***GCCGGGAATGACCGCGAG-3' and 5'- GTCA***CTCGAG***TTAA TTACTACCAAACATATCCTTGATCCAACC-3' were used to amplify *ponB* from E. coli MG1655 genomic DNA. The resulting PCR product was purified, digested with BamHI-HF and XhoI, and ligated into similarly digested pTU134 [*bla lacI*^{q} P_{lac}::*T18-amiA*] a derivative of pHC364 (Bendezú and de Boer, 2008).

pRY89

The plasmid pRY89 [*aph* P_{lac}::*T25-ponB*] was constructed as follows. The primers 5'-GGGTCGACTCTAGAA***GGATCC***GCCGGGAATGACCGCGAG-3' and 5'-GTCA***CTCGAG***TTAAT TACTACCAAACATATCCTTGATCCAACC-3' were used to amplify *ponB* from E. coli MG1655 genomic DNA. The resulting PCR product was purified, digested with BamHI-HF and XhoI, and ligated into similarly digested pTU135 [*aph* P_{lac}::*T25-amiA*] a derivative of pKT25 [*aph* P_{lac}::*T25-zip*] (Karimova *et al.*, 1998)..

pTU162

The plasmid pTU162 [*att*HK022 *bla lacI*^{q} P_{lac}::*slt*] was constructed as follows. The primers 5'-GTCA***CATATG***GAAAAAGCCAAACAAGTTACCTGGC-3' and 5'-GTCA***CTCGAG***GTAACGACGT CCCCATTCCGTG-3' were used to amplify *slt* from E. coli MG1655 genomic DNA. The resulting PCR product was purified, digested with NdeI and XhoI, and ligated into similarly digested pTU148 [*att*HK022 *bla lacI*^{q} P_{lac}::^{ss}*dsbA-mCherry*] (Peters *et al.*, 2011).

REFERENCES

Ashkenazy, H., Erez, E., Martz, E., Pupko, T., and Ben-Tal, N. (2010) ConSurf 2010: calculating evolutionary conservation in sequence and structure of proteins and nucleic acids. *Nucleic Acids Res* **38**: W529–W533.

Baba, T., Ara, T., Hasegawa, M., Takai, Y., Okumura, Y., Baba, M., *et al.* (2006) Construction of Escherichia coli K-12 in-frame, single-gene knockout mutants: the Keio collection. *Mol Syst Biol* **2**: 2006.0008.

Bateman, A. and Bycroft, M. (2000) The structure of a LysM domain from E. coli membrane-bound lytic murein transglycosylase D (MltD) *J Mol Biol* **299**:1113-1119.

Bendezú, F.O., and de Boer, P.A.J. (2008) Conditional lethality, division defects, membrane involution, and endocytosis in mre and mrd shape mutants of Escherichia coli. *J Bacteriol* **190**: 1792–1811.

Bernhardt, T.G., and de Boer, P.A.J. (2004) Screening for synthetic lethal mutants in Escherichia coli and identification of EnvC (YibP) as a periplasmic septal ring factor with murein hydrolase activity. *Molecular Microbiology* **52**: 1255–1269.

Bernhardt, T.G., and de Boer, P.A.J. (2005) SlmA, a nucleoid-associated, FtsZ binding protein required for blocking septal ring assembly over Chromosomes in E. coli. *Mol Cell* **18**: 555–564.

Cho, H., Uehara, T., and Bernhardt, T.G. (2014) Beta-lactam antibiotics induce a lethal malfunctioning of the bacterial cell wall synthesis machinery. *Cell* **159**: 1300–1311.

Datsenko, K.A., and Wanner, B.L. (2000) One-step inactivation of chromosomal genes in Escherichia coli K-12 using PCR products. *Proc Natl Acad Sci USA* **97**: 6640–6645.

de Boer, P.A., Crossley, R.E., and Rothfield, L.I. (1989) A division inhibitor and a topological specificity factor coded for by the minicell locus determine proper placement of the division septum in E. coli. *Cell* **56**: 641–649.

Guyer, M.S., Reed, R.R., Steitz, J.A., and Low, K.B. (1981) Identification of a sex-factor-affinity site in E. coli as gamma delta. *Cold Spring Harb Symp Quant Biol* **45 Pt 1**: 135–140.

Guzman, L.M., Belin, D., Carson, M.J., and Beckwith, J. (1995) Tight regulation, modulation, and high-level expression by vectors containing the arabinose PBAD promoter. *J Bacteriol* **177**: 4121–4130.

Haldimann, A., and Wanner, B.L. (2001) Conditional-replication, integration, excision, and retrieval plasmid-host systems for gene structure-function studies of bacteria. *J Bacteriol* **183**: 6384–6393.

Harz, H., Burgdorf, K., and Höltje, J.V. (1990) Isolation and separation of the glycan strands from murein of Escherichia coli by reversed-phase high-performance liquid chromatography. *Anal Biochem* **190**: 120–128.

Johnson, J.E., Lackner, L.L., Hale, C.A., and de Boer, P.A.J. (2004) ZipA is required for targeting of DMinC/DicB, but not DMinC/MinD, complexes to septal ring assemblies in Escherichia coli. *J Bacteriol* **186**: 2418–2429.

Karimova, G., Pidoux, J., Ullmann, A., and Ladant, D. (1998) A bacterial two-hybrid system based on a reconstituted signal transduction pathway. *Proc Natl Acad Sci USA* **95**: 5752–5756.

Kelley, L.A., Mezulis, S., Yates, C.M., Wass, M.N., and Sternberg, M.J.E. (2015) The Phyre2 web portal for protein modeling, prediction and analysis. *Nat Protoc* **10**: 845–858.

Lee, M., Hesek, D., Llarrull, L.I., Lastochkin, E., Pi, H., Boggess, B., and Mobashery, S. (2013) Reactions of all Escherichia coli lytic transglycosylases with bacterial cell wall. *J Am Chem Soc* **135**: 3311–3314.

Morlot, C., Uehara, T., Marquis, K.A., Bernhardt, T.G., and Rudner, D.Z. (2010) A highly coordinated cell wall degradation machine governs spore morphogenesis in Bacillus subtilis. *Genes Dev* **24**: 411–422.

Paradis-Bleau, C., Markovski, M., Uehara, T., Lupoli, T.J., Walker, S., Kahne, D.E., and Bernhardt, T.G. (2010) Lipoprotein cofactors located in the outer membrane activate bacterial cell wall polymerases. *Cell* **143**: 1110–1120.

Peters, N.T., Dinh, T., and Bernhardt, T.G. (2011) A fail-safe mechanism in the septal ring assembly pathway generated by the sequential recruitment of cell separation amidases and their activators. *J Bacteriol* **193**: 4973–4983.

Uehara, T., Dinh, T., and Bernhardt, T.G. (2009) LytM-domain factors are required for daughter cell separation and rapid ampicillin-induced lysis in Escherichia coli. *J Bacteriol* **191**: 5094–5107.

Uehara, T., Parzych, K.R., Dinh, T., and Bernhardt, T.G. (2010) Daughter cell separation is controlled by cytokinetic ring-activated cell wall hydrolysis. *EMBO J* **29**: 1412–1422.